Operational Curvature of the Heisenberg Cut

Exact diamond readout, a discrete Stokes law, and sharp action bounds for dissipative Zeno holonomy

Lluis Eriksson

10 August 2026

Abstract

The order of short operations is normally a microscopic detail. We show that a fixed degenerate measurement turns it into an operational curvature with an exact, macroscopic readout. Let $\mathcal{E}(X) = \sum_a P_a X P_a$ retain the block algebra $\mathcal{A} = \bigoplus_a \mathcal{B}(\mathcal{H}_a)$, and let $W_\sigma(\tau)$ be a word of short Hamiltonian kicks, each followed by the same nonselective pinching, in physical order σ. For any two permutations,

$$W_\sigma(\tau) - W_\pi(\tau) = -i\tau^2 \operatorname{ad}_{F_{\sigma,\pi}} \mathcal{E} + O_\diamond(\tau^3),$$

where $F_{\sigma,\pi}$ is the sum of $i[h_j, h_k]$, $h_j = \mathcal{E}(H_j)$, over pairwise inversions between the words. This is a discrete non-Abelian Stokes law. Its coefficient is exactly measurable:

$$\lim_{\tau\to 0} \tau^{-2} \left\| W_\sigma(\tau) - W_\pi(\tau) \right\|_\diamond = \operatorname{osc}_{\mathcal{A}}(F_{\sigma,\pi}),$$

with $\operatorname{osc}_{\mathcal{A}}(F)$ the largest spectral diameter of a block of F. Under first-order balance, all permutations have the same dissipator but different geometric Hamiltonians, and $H^\sigma_{\text{geo}} - H^\pi_{\text{geo}} = F_{\sigma,\pi}$; hence the local curvature integrates into distinct diffusive quantum Markov semigroups. We characterize contextual invisibility, the classical rank-one boundary, and the unavoidable inverse-success amplification under postselection. Every retained Hamiltonian modulo the block center is realizable by a balanced three-kick loop. For a qubit block we further prove the sharp resource law

$$\kappa \leq \frac{S^2}{m \tan(\pi/m)}, \qquad S_{\min} = \sqrt{m \tan(\pi/m)\, \kappa},$$

where S is retained action and $\kappa = \operatorname{osc}_{\mathcal{A}}(H_{\text{geo}})$; equality holds precisely at regular planar kick polygons. An integer-Pauli four-kick architecture simultaneously saturates the bound, produces $H_{\text{geo}} = 2Y$ in each qubit block, and supports primitive dissipation. Symbolic, semidefinite, and convergence certificates accompany the manuscript.

1 Question and main advance

The quantum Zeno effect constrains dynamics by frequent observations [1, 2]. Its modern formulations include open-system product limits [3], quasi-Zeno corrections [4], and non-Abelian holonomies generated by transported measurement subspaces [5, 6]. A fixed *degenerate* nonselective measurement contains a different resource: it destroys coherence between records while preserving a full matrix algebra inside each record. That internal algebra can remember the order of short kicks.

This paper asks a precise operational question. If two laboratories use the same Hamiltonians and the same fixed record projection but apply the Hamiltonians in different orders, what is the first completely bounded signature of the ordering, and when can it survive a many-cycle Zeno limit? The answer has three layers.

First, the pairwise inversions between two orderings carry a block Hamiltonian $F_{\sigma,\pi}$. It is a curvature because it is additive under concatenation of comparisons, changes sign under orientation reversal, and vanishes in every commutative retained algebra. Second, its operational size is not merely bounded: it equals a block spectral diameter and therefore determines the leading ancilla-assisted discrimination probability. Third, under a balanced diffusive scaling it becomes the exact difference between two effective Hamiltonians while the dissipative envelope stays fixed.

The strongest additional result is a sharp synthesis cost. In a qubit block, balanced retained kicks are the edges of a closed Euclidean polygon and geometric holonomy is four times its oriented area. The polygonal isoperimetric theorem then gives the exact minimum action for prescribed curvature and a fixed number of switches. This connects operator order, a completely bounded operational witness, and a sharp control resource law.

All statements are finite dimensional. We do not claim that commutator simulation, geometric phases, diamond discrimination, or the polygonal isoperimetric inequality are separately new. The proposed contribution is the exact chain

$$\begin{aligned}\text{inversion surface} &\longrightarrow \text{block curvature} \longrightarrow \text{diamond distinguishability}\\ &\longrightarrow \text{dissipative holonomy} \longrightarrow \text{optimal action.}\end{aligned}$$

2 Fixed records and ordered words

Let

$$\mathcal{H} = \bigoplus_{a=1}^{r} \mathcal{H}_a, \qquad \mathcal{A} = \bigoplus_{a=1}^{r} \mathcal{B}(\mathcal{H}_a), \qquad \mathcal{E}(X) = \sum_{a=1}^{r} P_a X P_a.$$

The pinching $\mathcal{E}$ is a trace-preserving, unital conditional expectation onto $\mathcal{A}$. For Hermitian Hamiltonians $H_1, \dots, H_m$, put

$$\mathcal{U}_{j,\tau}(X) = e^{-i\tau H_j} X e^{i\tau H_j}, \qquad h_j = \mathcal{E}(H_j), \qquad A_j = \mathrm{ad}_{h_j}.$$

For a permutation $\sigma = (\sigma_1, \dots, \sigma_m)$, with σ_1 applied first, define

$$W_\sigma(\tau) = \mathcal{E}\mathcal{U}_{\sigma_m,\tau}\mathcal{E} \cdots \mathcal{E}\mathcal{U}_{\sigma_1,\tau}\mathcal{E}. \tag{1}$$

Distances between maps use the completely bounded trace norm $\|\cdot\|_\diamond$ [7]. Write

$$\mathrm{osc}_{\mathcal{A}}(F) = \max_a \{\lambda_{\max}(P_a F P_a) - \lambda_{\min}(P_a F P_a)\} \tag{2}$$

for a block-diagonal Hermitian F. Thus $\mathrm{osc}_{\mathcal{A}}(F) = 0$ exactly when F lies in the center $Z(\mathcal{A}) = \bigoplus_a \mathbb{C}P_a$.

For two permutations, let $\mathrm{Inv}(\sigma, \pi)$ contain the unordered label pairs whose relative order differs. Orient every such pair (j,k) so that j occurs before k in σ, and define the inversion flux

$$F_{\sigma,\pi} = \sum_{(j,k)\in\mathrm{Inv}(\sigma,\pi)} i[h_j, h_k]. \tag{3}$$

It is Hermitian and belongs to $\mathcal{A}$.

3 A discrete non-Abelian Stokes law

Theorem 3.1 (permutation curvature)**.** *Let $S = \sum_j \|H_j\|$. For every pair of permutations,*

$$W_\sigma(\tau) - W_\pi(\tau) = -i\tau^2\, \mathrm{ad}_{F_{\sigma,\pi}} \mathcal{E} + R_{\sigma,\pi}(\tau), \tag{4}$$

with the dimension-free bound

$$\|R_{\sigma,\pi}(\tau)\|_\diamond \le \frac{8}{3} S^3 |\tau|^3. \tag{5}$$

Moreover $F_{\sigma,\pi} = -F_{\pi,\sigma}$ and

$$F_{\sigma,\pi} + F_{\pi,\rho} = F_{\sigma,\rho} \quad \textit{modulo } Z(\mathcal{A}). \tag{6}$$

In fact equality holds for the representatives in (3).

Proof. Restricted to $\mathcal{A}$, a factor has Taylor expansion

$$\mathcal{E}\mathcal{U}_{j,\tau}\mathcal{E} = I - i\tau A_j - \frac{\tau^2}{2}\mathcal{E}\,\mathrm{ad}^2_{H_j}\,\mathcal{E} + O_\diamond(\tau^3).$$

Every term involving only one label is independent of the permutation. If j is earlier than k, multiplication contributes $-\tau^2 A_k A_j$. Reversing that pair changes the coefficient by

$$-A_k A_j + A_j A_k = [A_j, A_k] = \mathrm{ad}_{[h_j,h_k]} = -i\,\mathrm{ad}_{i[h_j,h_k]}\,.$$

Summing the inverted pairs proves (4).

For the remainder, differentiate the complete word three times. Pinchings and unitary channels have diamond norm one, while $\left\|\mathrm{ad}_{H_j}\right\|_\diamond \leq 2\,\|H_j\|$. The multinomial sum of third derivatives is at most $(2S)^3$. Taylor's integral remainder for one word is at most $\frac{4}{3}S^3|\tau|^3$; subtracting two words gives (5). Antisymmetry is immediate. Additivity follows either pairwise or from the identity in Theorem 5.1 below. □

Equation (4) is discrete Stokes in a literal combinatorial sense: adjacent transpositions are elementary plaquettes, an inversion set is a two-chain spanning two paths through the permutation graph, and $F_{\sigma,\pi}$ is its non-Abelian flux. Different spanning sequences give the same second-order boundary observable.

Corollary 3.2 (adjacent swap)**.** *If two words differ only by swapping adjacent kicks j then k, their curvature is $i[h_j, h_k]$. Hence second-order order sensitivity is absent for all words if and only if every $[h_j, h_k]$ is block-central.*

4 Exact diamond readout

The expansion becomes operational only after its coefficient is evaluated in the same stabilized norm used to distinguish channels.

Lemma 4.1 (exact norm of a retained derivation)**.** *For block-diagonal Hermitian F,*

$$\|-i\,\mathrm{ad}_F\,\mathcal{E}\|_\diamond = \mathrm{osc}_{\mathcal{A}}(F). \tag{7}$$

No ancilla is needed to attain the lower bound.

Proof. Choose a block-central $Z = \sum_a z_a P_a$ whose scalar in each block is the midpoint of the extreme eigenvalues of $F_a = P_a F P_a$. Then $\mathrm{ad}_F\,\mathcal{E} = \mathrm{ad}_{F-Z}\,\mathcal{E}$, and

$$\|-i\,\mathrm{ad}_F\,\mathcal{E}\|_\diamond \leq 2\,\|F - Z\| = \max_a(\lambda_{\max}(F_a) - \lambda_{\min}(F_a)).$$

For a maximizing block, let u_+ and u_- be extreme eigenvectors and take $X = |u_+\rangle\langle u_-|$. It has trace norm one, $\mathcal{E}(X) = X$, and

$$\|[F, X]\|_1 = (\lambda_{\max} - \lambda_{\min})\,\|X\|_1\,.$$

This gives the matching lower bound. □

Theorem 4.2 (operational curvature coefficient)**.** *For any two orderings,*

$$\lim_{\tau\to 0}\frac{\|W_\sigma(\tau) - W_\pi(\tau)\|_\diamond}{\tau^2} = \mathrm{osc}_{\mathcal{A}}(F_{\sigma,\pi}). \tag{8}$$

With equal priors, their optimal single-use success probability satisfies

$$p_{\mathrm{succ}}(\tau) = \frac{1}{2} + \frac{\tau^2}{4}\,\mathrm{osc}_{\mathcal{A}}(F_{\sigma,\pi}) + O(\tau^3). \tag{9}$$

Thus curvature is operationally invisible at second order exactly when its flux is block-central.

Proof. Divide (4) by τ^2, use (5), and apply Lemma 4.1. Equation (9) is the channel version of Helstrom discrimination [8]. $\square$

This exact equality is stronger than a norm estimate. It identifies the gauge freedom: adding independent scalar energies in the record blocks changes neither curvature nor any retained operational test.

5 Balanced integration into dissipative holonomy

Define the leakage Gramians on $\mathcal{A}$ by

$$K_j = \mathcal{E}\,\mathrm{ad}_{H_j}(1-\mathcal{E})\,\mathrm{ad}_{H_j}\,\mathcal{E} = C_j^* C_j, \qquad C_j = (1-\mathcal{E})\,\mathrm{ad}_{H_j}|_{\mathcal{A}}. \tag{10}$$

A family is balanced when $\sum_j A_j = 0$, equivalently $\sum_j h_j \in Z(\mathcal{A})$. For an ordering σ, set

$$H^\sigma_{\mathrm{geo}} = -\frac{i}{2}\sum_{s>r}[h_{\sigma_s}, h_{\sigma_r}], \qquad \mathcal{L}_\sigma = -\frac{1}{2}\sum_j K_j - i\,\mathrm{ad}_{H^\sigma_{\mathrm{geo}}}. \tag{11}$$

The first term is the restriction of a GKLS dissipator with jumps $P_b H_j P_a$, $a \neq b$; see [12] for the direct product theorem and fixed-algebra analysis.

Theorem 5.1 (integration identity)**.** *For a balanced family and any permutation σ,*

$$W_\sigma(\sqrt{t/n})^n \longrightarrow e^{t\mathcal{L}_\sigma}\mathcal{E} \quad \text{in diamond norm at rate } O(n^{-1/2}). \tag{12}$$

More precisely, with

$$S = \sum_j \|H_j\|, \qquad g = 2\sum_j \|H_j\|^2 + 2\left\|H^\sigma_{\mathrm{geo}}\right\|,$$

one has

$$\left\|W_\sigma(\sqrt{t/n})^n - e^{t\mathcal{L}_\sigma}\mathcal{E}\right\|_\diamond \leq \frac{4S^3t^{3/2}}{3\sqrt{n}} + \frac{g^2t^2}{2n}e^{gt/n}. \tag{13}$$

For any two orderings,

$$H^\sigma_{\mathrm{geo}} - H^\pi_{\mathrm{geo}} = F_{\sigma,\pi}, \qquad \mathcal{L}_\sigma - \mathcal{L}_\pi = -i\,\mathrm{ad}_{F_{\sigma,\pi}}. \tag{14}$$

Consequently,

$$\lim_{t\downarrow 0}\frac{\left\|e^{t\mathcal{L}_\sigma}\mathcal{E} - e^{t\mathcal{L}_\pi}\mathcal{E}\right\|_\diamond}{t} = \mathrm{osc}_{\mathcal{A}}(F_{\sigma,\pi}), \tag{15}$$

and for all $t \geq 0$,

$$\left\|e^{t\mathcal{L}_\sigma}\mathcal{E} - e^{t\mathcal{L}_\pi}\mathcal{E}\right\|_\diamond \leq t\ \mathrm{osc}_{\mathcal{A}}(F_{\sigma,\pi}). \tag{16}$$

Proof. The expansion of a balanced word is $\mathcal{E} + \tau^2\mathcal{L}_\sigma\mathcal{E} + R_\tau$, with $\|R_\tau\|_\diamond \leq \frac{4}{3}S^3|\tau|^3$. The jump representation following (11) implies $\|\mathcal{L}_\sigma\|_\diamond \leq g$. Taylor's integral formula gives

$$\left\|e^{s\mathcal{L}_\sigma}\mathcal{E} - (\mathcal{E} + s\mathcal{L}_\sigma\mathcal{E})\right\|_\diamond \leq \frac{1}{2}s^2g^2e^{sg}.$$

Telescoping n powers of two contractions, with $s = t/n$ and $\tau = \sqrt{s}$, proves (13). Comparing the pair terms in (11) gives (14); it also proves the cocycle identity in Theorem 3.1. Equation (15) follows from differentiability and Lemma 4.1. Duhamel's formula and contractivity of both quantum Markov semigroups give (16). $\square$

Thus order is not a vanishing correction. At diffusive scale it survives as an $O(1)$ Hamiltonian difference embedded inside a common irreversible envelope. Full reversal sends H^σ_{geo} to $-H^\sigma_{\mathrm{geo}}$ while leaving $\sum_j K_j$ unchanged.

6 Context, cut transport, and postselection

Operational visibility depends on what can be prepared and read out around the cut. Let $\mathcal{U}$ be a common preprocessing channel and $\mathcal{T}$ a common postprocessing channel. Define the contextual curvature

$$\kappa_{\mathcal{T},\mathcal{U}}(F) = \|\mathcal{T}(-i\,\mathrm{ad}_F)\mathcal{E}\mathcal{U}\|_\diamond \,. \tag{17}$$

Proposition 6.1 (contextual Heisenberg criterion)**.** *The two words are invisible to second order in the context $(\mathcal{T},\mathcal{U})$ if and only if*

$$\mathcal{T}\,\mathrm{ad}_F\,\mathcal{E}\mathcal{U} = 0. \tag{18}$$

Equivalently, for every accessible Heisenberg observable O and every accessible input X,

$$\mathrm{Tr}[\mathcal{T}^*(O)(-i[F,\mathcal{E}\mathcal{U}(X)])] = 0. \tag{19}$$

If this fails, a finite ancilla-assisted binary test witnesses the ordering with leading coefficient $\kappa_{\mathcal{T},\mathcal{U}}(F)$.

This formulation separates structural curvature from accessible curvature. A noncentral F can be hidden by a downstream dephasing or by an input restriction, but that is contextual erasure, not flatness of the retained algebra. It is also the natural finite-dimensional condition for moving the operational Heisenberg cut through a circuit [11].

Postselection can amplify small curvature. Let $\mathcal{J}$ be a trace-nonincreasing success branch and suppose both success probabilities are at least $\eta > 0$ on the tested input. If $\rho_\sigma^{\mathrm{suc}}$ and ρ_π^{suc} are the normalized conditional states, then

$$\frac{1}{2}\,\|\rho_\sigma^{\mathrm{suc}} - \rho_\pi^{\mathrm{suc}}\|_1 \le \min\left\{1, \frac{\|\mathcal{J}(W_\sigma - W_\pi)\|_\diamond}{\eta}\right\}. \tag{20}$$

The factor $1/\eta$ cannot be replaced uniformly by a constant: rare branches can carry an $O(1)$ normalized contrast while their unconditioned weight is $O(\eta)$. Therefore postselected curvature claims must report the success floor.

7 Universality and the three-kick threshold

Curvature is not confined to special Pauli examples.

Theorem 7.1 (curvature universality)**.** *Let $F \in \mathcal{A}$ be Hermitian and traceless in every block. There exist block-diagonal Hermitian $h, g \in \mathcal{A}$ with*

$$F = i[h, g]. \tag{21}$$

Hence every retained Hamiltonian modulo $Z(\mathcal{A})$ is generated by the balanced four-kick loop $(h, g, -h, -g)$. It is also generated by a balanced three-kick loop after rescaling. Two balanced kicks always have zero curvature, so three is minimal.

Proof. Work blockwise. By Schur–Horn, a traceless Hermitian matrix has a basis in which its diagonal is zero [9]. Choose a diagonal $h = \mathrm{diag}(\lambda_1, \ldots, \lambda_d)$ with distinct entries and set

$$g_{jk} = \frac{-iF_{jk}}{\lambda_j - \lambda_k} \quad (j \neq k), \qquad g_{jj} = 0.$$

Then g is Hermitian and $i[h, g] = F$. Direct substitution into (11) shows that $(h, g, -h, -g)$ has $H_{\mathrm{geo}} = i[h, g] = F$. The three-kick loop $(h, g, -h - g)$ has $H_{\mathrm{geo}} = \frac{i}{2}[h, g]$, so scaling one generator by two gives F. A balanced two-kick loop is $(h, -h)$ modulo the center, and its commutator vanishes. ∎

Corollary 7.2 (classical boundary). *If every record block is rank one, then $\mathcal{A}$ is commutative, $F_{\sigma,\pi} = 0$, and $H^{\sigma}_{\text{geo}} = 0$ for every word. The second-order limit can still mix record probabilities, but it carries no non-Abelian curvature.*

Degeneracy is therefore not a quantitative enhancement; it is the algebraic threshold between classical record diffusion and coherent geometric response.

8 Sharp qubit action law

Fix one two-dimensional block. Remove block-scalar parts and write

$$h_j = \boldsymbol{v}_j \cdot \boldsymbol{\sigma}, \qquad \sum_{j=1}^{m} \boldsymbol{v}_j = 0, \qquad S = \sum_{j=1}^{m} \|h_j\| = \sum_j |\boldsymbol{v}_j|. \tag{22}$$

The vectors are the ordered edges of a closed polygon in $\mathbb{R}^3$. Let $\boldsymbol{A}$ be its oriented area vector,

$$\boldsymbol{A} = \frac{1}{2} \sum_{j<k} \boldsymbol{v}_j \times \boldsymbol{v}_k. \tag{23}$$

Pauli commutation gives

$$H_{\text{geo}} = \boldsymbol{g} \cdot \boldsymbol{\sigma}, \qquad \boldsymbol{g} = -2\boldsymbol{A}, \qquad \kappa := \operatorname{osc}_{\mathcal{A}}(H_{\text{geo}}) = 4|\boldsymbol{A}|. \tag{24}$$

Theorem 8.1 (sharp action–curvature inequality). *Every balanced m-kick qubit loop, $m \geq 3$, satisfies*

$$\boxed{\kappa \leq \frac{S^2}{m \tan(\pi/m)}} \tag{25}$$

or equivalently

$$S \geq S_{\min}(m, \kappa) := \sqrt{m \tan(\pi/m)\, \kappa}. \tag{26}$$

The constant is optimal. Equality holds for a planar regular m-gon, and every Pauli direction of H_{geo} is attainable by rotating its plane.

Proof. Projection onto the plane orthogonal to $\boldsymbol{A}$ preserves the oriented area $|\boldsymbol{A}|$ and cannot increase edge lengths. The polygonal isoperimetric theorem states that a planar m-gon of perimeter at most S has area

$$|\boldsymbol{A}| \leq \frac{S^2}{4m \tan(\pi/m)},$$

with equality for the regular polygon [10]. Multiply by four and use (24). Rotational covariance gives all target directions. □

Corollary 8.2 (switch price). *Three kicks are the shortest nonflat loop and require*

$$S \geq 3^{3/4}\sqrt{\kappa}.$$

At fixed κ, allowing arbitrarily many kicks lowers the infimum only to

$$\lim_{m\to\infty} S_{\min}(m, \kappa) = \sqrt{\pi\kappa}. \tag{27}$$

Thus additional switching has a finite continuum benefit and cannot make curvature free.

The law is invariant under block-scalar energy shifts and concerns only retained action. Off-block couplings may be chosen independently to tune dissipation, subject to their own laboratory cost.

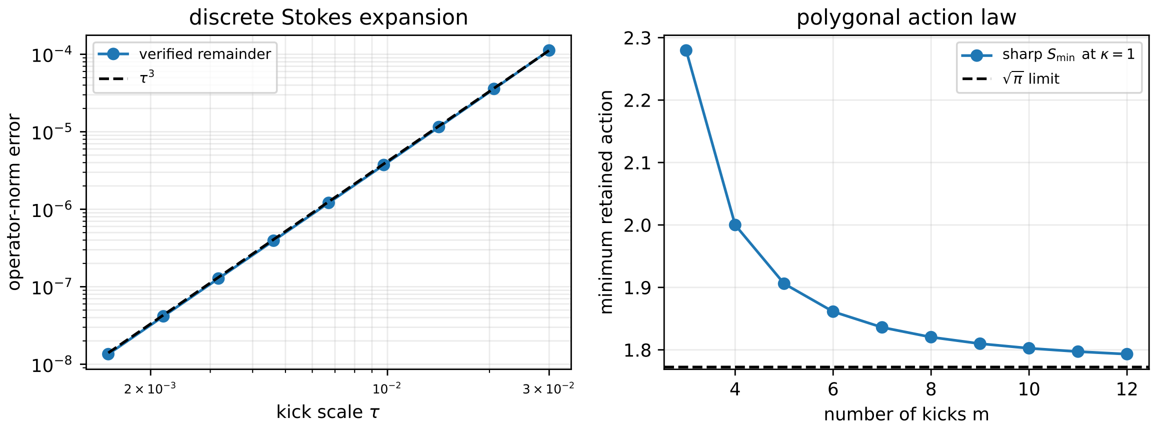

Figure 1: Left: after subtracting the predicted quadratic curvature map, the permutation-word residual scales as τ^3. Right: the exact minimum retained action for unit curvature approaches $\sqrt{\pi}$ as the number of kicks grows. Points are regular polygons and therefore equality cases, not numerical optimizers.

9 Exact architecture and reproducible audit

Consider two qubit blocks and the four full Hamiltonians

$$H_j = \begin{pmatrix} h_j & V_j \\ V_j^* & h_j \end{pmatrix}, \qquad (h_1, h_2, h_3, h_4) = (X, Z, -X, -Z), \quad (V_1, V_2, V_3, V_4) = (I, X, Z, Y). \tag{28}$$

The retained loop is balanced. In either block,

$$H_{\text{geo}} = 2Y, \qquad \kappa = 4, \qquad S = 4 = \sqrt{4\tan(\pi/4)\,4}. \tag{29}$$

Thus the square exactly saturates Theorem 8.1. Reversal produces $-2Y$. The forward–reverse flux is $4Y$ and its exact diamond coefficient is 8. The off-block couplings form a primitive leakage frame: the half-Gram spectrum is $0, 4, 4, 4, 4, 4, 4, 8$, so dissipation has a one-dimensional fixed algebra and gap 4.

The accompanying deterministic replay performs four independent checks:

(i) a semidefinite program verifies $\|-i\,\mathrm{ad}_F\,\mathcal{E}\|_\diamond = \mathrm{osc}_{\mathcal{A}}(F)$;

(ii) all 24 permutations verify $H^\sigma_{\text{geo}} - H^\pi_{\text{geo}} = F_{\sigma,\pi}$ to 10^{-12};

(iii) small-τ word differences have a fitted cubic residual;

(iv) regular polygons for $3 \le m \le 12$ saturate (26), while 1000 seeded closed random polygons obey it.

A separate SymPy script certifies the exact Pauli identities and equality in (29).

10 Interpretation, limits, and falsifiability

The measurement does two logically distinct things. Its off-block sector converts excursions into a GKLS dissipator. Its retained noncommutative sector converts order into curvature. The two contributions coexist at the same τ^2 scale yet can be engineered independently: changing the $V_j = P_a H_j P_b$ leaves $F_{\sigma,\pi}$ fixed, while changing retained h_j at fixed off-block couplings changes holonomy without changing the leakage Gram formula.

Table 1: Exact and independently replayed claims for (28).

Quantity	Exact value	Audit route
Forward H_{geo}	$2Y \oplus 2Y$	SymPy
Reverse H_{geo}	$-2Y \oplus -2Y$	SymPy
Single-orientation κ	4	block spectrum
Retained action S	4	exact Pauli norms
Action lower bound	4	Theorem 8.1
Forward–reverse coefficient	8	diamond SDP
Permutation Stokes error	$< 10^{-12}$	all 24 orders
Leakage-frame gap	4	exact characteristic polynomial

The theory has clear failure modes. Curvature disappears for rank-one records, for pairwise commuting retained kicks, or when every inversion flux is block-central. A nonzero structural flux can still be inaccessible in a restricted preparation/readout context. Balance is essential for the diffusive interpretation: without it an $O(\tau)$ ballistic motion dominates. The sharp action law is special to a two-dimensional block; higher-rank optimal synthesis becomes a noncommutative matrix isoperimetric problem and is left open. The finite-dimensional hypothesis also avoids domain questions for unbounded generators.

The main claims are directly falsifiable. A counterexample to (4) would be an ordered word whose normalized difference does not converge to the inversion commutator. A counterexample to (8) would separate the diamond norm of a retained derivation from its largest block spectral diameter. A counterexample to (25) would be a closed qubit kick polygon enclosing more area than the regular polygon with the same perimeter and number of edges. The supplied tests address representative cases but do not replace the analytic proofs.

11 Conclusion

A fixed record projection can endow the space of operation orderings with an observable non-Abelian curvature. Pairwise inversions supply a discrete Stokes flux; its exact diamond norm is a block spectral diameter; balance integrates it into a macroscopic dissipative holonomy; and in a qubit block its synthesis cost is governed sharply by polygonal isoperimetry. This identifies a concrete physical status for a movable operational cut: two descriptions are equivalent only when the curvature transported across the cut is inaccessible in the chosen context. Degenerate records are the minimal quantum substrate, three balanced kicks are the minimal loop, and regular polygons are the optimal finite-switch controls.

Data and code availability

The reproducibility archive contains the LaTeX source, deterministic NumPy/SciPy implementation, a general-map diamond-norm SDP in CVXPY, an exact SymPy certificate, JSON outputs, figure source, a claim ledger, and SHA-256 manifest. No external data are used.

AI-assistance disclosure

The author used OpenAI Codex for literature triage, symbolic and numerical code, proof stress-testing, and manuscript drafting. The mathematical claims are presented with explicit proofs and reproducible certificates; responsibility for the submitted content remains with the author.

A Second-order word algebra

For completeness, we record the coefficient calculation behind both the local Stokes law and the product generator. On $\mathcal{A}$, put $D_j = \mathrm{ad}_{H_j}$. Taylor expansion gives

$$T_j(\tau) := \mathcal{E} e^{-i\tau D_j} \mathcal{E} = I - i\tau A_j - \frac{\tau^2}{2}(A_j^2 + K_j) + O_\diamond(\tau^3), \tag{30}$$

because $\mathcal{E} D_j^2 \mathcal{E} = A_j^2 + K_j$. Multiplying in order σ yields

$$W_\sigma(\tau)|_{\mathcal{A}} = I - i\tau \sum_j A_j - \frac{\tau^2}{2} \sum_j (A_j^2 + K_j) - \tau^2 \sum_{s>r} A_{\sigma_s} A_{\sigma_r} + O_\diamond(\tau^3). \tag{31}$$

If $\sum_j A_j = 0$, then

$$\sum_{s>r} A_{\sigma_s} A_{\sigma_r} = -\frac{1}{2} \sum_j A_j^2 + \frac{1}{2} \sum_{s>r} [A_{\sigma_s}, A_{\sigma_r}], \tag{32}$$

and (11) follows. Subtracting (31) for two orders cancels every diagonal term and leaves precisely the inverted commutators. This also shows why leakage affects the common dissipator but not permutation curvature at second order.

The full-space GKLS extension of the dissipative part can be checked directly. For $J_{j,ba} = P_b H_j P_a$, $a \neq b$, define

$$\widetilde{\mathcal{D}}(X) = \sum_{j, a\neq b} \left(J_{j,ba} X J_{j,ba}^* - \frac{1}{2} \{ J_{j,ba}^* J_{j,ba}, X \} \right). \tag{33}$$

Restricting (33) to $\mathcal{A}$ gives $-\frac{1}{2}\sum_j K_j$. Adding $-i[H_{\mathrm{geo}}^\sigma, X]$ proves that $\mathcal{L}_\sigma$ generates a completely positive trace-preserving semigroup. The elementary bounds

$$\left\| \widetilde{\mathcal{D}} \right\|_\diamond \le 2 \sum_j \|H_j\|^2, \qquad \left\| -i\, \mathrm{ad}_{H_{\mathrm{geo}}^\sigma} \right\|_\diamond \le 2 \left\| H_{\mathrm{geo}}^\sigma \right\|$$

justify the constant g in (13).

B Normalization under a rare branch

Let $A, B \ge 0$ be two subnormalized branch outputs with $p = \operatorname{Tr} A \ge \eta$ and $q = \operatorname{Tr} B \ge \eta$. Then

$$\|A/p - B/q\|_1 \le \|(A - B)/p\|_1 + \|B(1/p - 1/q)\|_1 \tag{34}$$

$$= \frac{\|A - B\|_1}{p} + \frac{|p - q|}{p} \le \frac{2\,\|A - B\|_1}{\eta}, \tag{35}$$

because $|p - q| \le \|A - B\|_1$. Dividing by two and maximizing over the tested input proves (20). To see sharpness of the scaling, take classical subnormalized outputs $A = \eta|0\rangle\langle 0|$ and $B = \eta|1\rangle\langle 1|$. Their unconditioned trace distance is η, while the conditional distance is one.

C Verifier conventions

The numerical code uses column-major vectorization,

$$\mathrm{vec}(AXB) = (B^\mathsf{T} \otimes A)\, \mathrm{vec}(X).$$

The SDP evaluates the completely bounded trace norm of a general Hermiticity-preserving map from its Choi matrix, not from a state-only surrogate. Absolute tolerances are 2×10^{-6} for the SDP equality and 10^{-12} for algebraic matrix identities. The random polygon test uses seed 20260810 and is supplementary evidence only; the sharp inequality rests on Theorem 8.1.

References

[1] B. Misra and E. C. G. Sudarshan, "The Zeno's paradox in quantum theory," *J. Math. Phys.* **18**, 756–763 (1977). doi:10.1063/1.523304.

[2] P. Facchi and S. Pascazio, "Quantum Zeno dynamics: mathematical and physical aspects," *J. Phys. A* **41**, 493001 (2008). doi:10.1088/1751-8113/41/49/493001.

[3] S. Becker, N. Datta, and R. Salzmann, "Quantum Zeno effect for open quantum systems," *Ann. Henri Poincaré* **22**, 3795–3840 (2021). doi:10.1007/s00023-021-01075-8.

[4] T. J. Elliott and V. Vedral, "Quantum quasi-Zeno dynamics: transitions mediated by frequent projective measurements," *Phys. Rev. A* **94**, 012118 (2016). doi:10.1103/PhysRevA.94.012118.

[5] D. Burgarth, P. Facchi, V. Giovannetti, H. Nakazato, S. Pascazio, and K. Yuasa, "Non-Abelian phases from quantum Zeno dynamics," *Phys. Rev. A* **88**, 042107 (2013). doi:10.1103/PhysRevA.88.042107.

[6] S. Lanka and T. A. Brun, "Holonomic quantum computation via continuous quantum measurement," arXiv:2510.06725 (2025). arXiv:2510.06725.

[7] J. Watrous, *The Theory of Quantum Information*, Cambridge University Press (2018). doi:10.1017/9781316848142.

[8] C. W. Helstrom, *Quantum Detection and Estimation Theory*, Academic Press (1976).

[9] R. A. Horn and C. R. Johnson, *Matrix Analysis*, 2nd ed., Cambridge University Press (2013).

[10] L. Fejes Tóth, *Regular Figures*, Pergamon Press (1964).

[11] L. Eriksson, "Operational Transport of the Heisenberg Cut in Finite Quantum Chains," manuscript (2026).

[12] L. Eriksson, "Balanced Block Measurements Generate Dissipative Quantum Holonomy," manuscript (2026).